MicroRNAs Are Involved in the Hypothalamic Leptin Sensitivity

Adel Derghal, Mehdi Djelloul, Myriam Azzarelli, Sébastien Degonon, Franck Tourniaire, Jean-Francois Landrier, Lourdes Mounien

HAL Id: hal-02010517

https://amu.hal.science/hal-02010517

Submitted on 7 Feb 2019

MicroRNAs Are Involved in the Hypothalamic Leptin Sensitivity

Adel Derghal[a], Mehdi Djelloul[b], Myriam Azzarelli[a], Sébastien Degonon[a], Franck Tourniaire[a,c], Jean-François Landrier[a,c] and Lourdes Mounien[a]

[a]Aix Marseille Univ, INSERM, INRA, C2VN, Marseille, France; [b]Department of Cell and Molecular Biology, Karolinska Institute, Stockholm, Sweden; [c]CriBioM, Criblage Biologique Marseille, Faculté de Médecine de la Timone, Marseille, France

Abbreviations: ARC, arcuate nucleus; CNS, central nervous system; HFD, high fat diet; Irs-2, Insulin receptor 2; LepR, leptin receptor; MC4-R, melanocortin receptor 4; miRNAs, micro ribonucleic acid; PDKO, Pomc Dicer knock-out, POMC, pro-opiomelanocortin; 3'UTR, 3' untranslated region.

Contact: Lourdes Mounien

lourdes.mounien@univ-amu.fr

C2VN–INSERM 1263–INRA 1260–AMU

Faculté de Médecine

27, boulevard Jean Moulin

13385 Marseille Cedex 5

France

Phone: +33-(0)491324284, Fax: +33(0)491254336

KEYWORDS

pro-opiomelanocortin, microRNA, hypothalamus, brown adipose tissue, leptin, DICER

ABSTRACT

The central nervous system monitors modifications in metabolic parameters or hormone levels (leptin) and elicits adaptive responses such as food intake and glucose homeostasis regulation. Particularly, within the hypothalamus, pro-opiomelanocortin (POMC) neurons are crucial regulators of energy balance. Consistent with a pivotal role of the melanocortin system in the control of energy homeostasis, disruption of the *Pomc* gene causes hyperphagia and obesity. *Pomc* gene expression is tightly controlled by different mechanisms. Interestingly, recent studies pointed to a key role for micro ribonucleic acid (miRNAs) in the regulation of gene expression. However, the role of miRNAs in the leptin sensitivity in hypothalamic melanocortin system has never been assessed. We developed a transgenic mouse model (PDKO) with a partial deletion of the miRNA processing enzyme DICER specifically in POMC neurons. PDKO mice exhibited a normal body weight but a decrease of food intake. Interestingly, PDKO mice had decreased metabolic rate by reduction of VO_2 consumption and CO_2 production which could explain that PDKO mice have normal weight while eating less. Interestingly, we observed an increase of leptin sensitivity in the POMC neurons of PDKO mice which could explain the decrease of food intake in this model. We also observed an increase in the expression of genes involved in the function of brown adipose tissue that is in polysynaptic contact with the POMC neurons. In summary, these results support the hypothesis that Dicer-derived miRNAs may be involved in the effect of leptin on POMC neurons activity.

Introduction

The hypothalamus is involved in the monitoring of the modifications in metabolic parameters (blood glucose and lipids) and/or hormones (insulin or leptin) and elicits adaptive responses like food intake regulation or autonomic nervous system modulation [1]. Within the arcuate nucleus (ARC) of the hypothalamus, pro-opiomelanocortin (POMC) neurons are the first to respond to the circulating signals of hunger and satiety such as leptin, insulin, ghrelin or glucose [1–8]. In accordance with the pivotal role of the melanocortin system in the control of food intake, it has been shown that the disruption of the POMC and melanocortin receptor 4 (MC4R) genes in mice models causes obesity [9,10]. In humans, obesity can result from mutation in the melanocortin system pathway including, leptin receptor deficiency, POMC deficiency, and MC3/4R deficiency [11].

Recently, several studies describe mechanisms that link energy homeostasis defect to dysfunction of POMC neurons activity as leptin signaling impairement [12–14] or autopaghy processes [15]. In this context, the appropriate responses to hormonal and nutritional signals by relevant neuronal subsets including POMC neurons are achieved through the modulation of intracellular signaling pathways involved in the transcriptional regulation of specific genes. Several studies have shown that *Pomc* gene expression is tightly controlled by different mechanisms. Particularly, epigenetic mechanisms such as histone modifications or DNA methylation were shown to modulate *Pomc* gene activity under different nutritional status [16–19]. For instance, hypomethylation of *Pomc* promoter markers in fetal hypothalami was identified after maternal undernutrition in the ovine [16]. It also been shown a long-term effect of maternal high fat diet (HFD) on CpG methylation of the *Pomc* promoter in the offspring [19].

Interestingly, recent studies also pointed to a key role for micro ribonucleic acid (miRNAs) in the regulation of gene expression [20,21]. The miRNAs operate at the RNA level and play predominantly inhibitory regulatory roles by binding to *cis*-element in the 3' untranslated region (3'UTR) of message-encoding RNAs [20,21]. Several studies have suggested that

miRNAs play a critical role in lipid and glucid metabolism, adipogenesis, obesity-related diseases and also in the central control of energy homeostasis [1,22–24]. For instance, the neuron-specific deletion of *Dicer*, a critical enzyme involved in miRNAs maturation, induced serious obesity [25]. In the hypothalamus, adult deletion of *Dicer* in the ARC caused hyperphagia and obesity [26]. In addition, the relevance of miRNAs in the function of melanocortin pathways has been recently highlighted by the deletion of *Dicer* in POMC-expressing cells which led to obesity associated with a postnatal ablation of POMC neurons [27,28].

The identification of particular hypothalamic miRNAs implicated in the control of energy balance has been done by several groups. Crepin et al. exhibited the differential expression for miR-200a, miR-200b and miR-429 in the hypothalamus from leptin-deficient *ob/ob* mice versus non obese animals [29]. Furthermore, this group showed that miR-200a was also increased in the hypothalamus of leptin receptor (LepR) deficient *db/db* mice [29]. *In silico* and luciferase activity studies indicated that Insulin receptor substrate 2 (Irs-2) and LepR are direct targets of miR-200a [29]. The hypothalamic silencing of miR-200a increased the expression level of LepR and Irs-2 mRNA and reduced body weight gain in *ob/ob* mice model [29]. In this context, we have recently found that leptin modulated for the expression of miRNAs, *i.e.* miR-383, miR-384-3p and miR-488, that target POMC mRNA in the hypothalamus [30]. The intraperitoneal injection of leptin down-regulated the expression of these miRNAs of interest in the hypothalamus of *ob/ob* mice showing the involvement of leptin in the expression of mir-383, mir-384-3p and mir-488 [30].

Altogether, above collected data strongly suggest an interaction between miRNAs and leptin signaling in the hypothalamus. However, the role of miRNAs in the leptin sensitivity in hypothalamic melanocortin system has never been assessed. Because the deletion of the two alleles of *Dicer* in POMC-expressing cells led to a postnatal ablation of POMC neurons [27,28], we used a mice model where one allele of *Dicer* gene in the POMC cells was inactivated

(PDKO). We used this model in order to clarify the implication of the miRNAs in the leptin

action at the hypothalamus level.

Results

Metabolic studies

Because the deletion of the two alleles of *Dicer* in POMC-expressing cells led to a postnatal ablation of POMC neurons [27,28], we used in our study a mice model with the inactivation of one allele of *Dicer* gene. To generate PDKO mice (*Dicer^{loxP/+}; PomcCre*), we crossbred mice carrying conditional *Dicer* alleles [31] with mice expressing Cre recombinase specifically in POMC expressing-cells [32]. The PDKO mice were born phenotypically normal and at the expected genetic ratio (supplementary Figure 1). There was no significant difference in body weight between PDKO and control male mice fed with a normal chow (Figure 1A).

At the age of 12 weeks, cumulative food intake was significantly lower in PDKO mice compared to control animals (Figure 1B). The meal microstructural analysis of eating behavior in PDKO and control mice was performed for the light and dark (active) phases of the day cycle. The number and duration of meals as well as the intermeal period were similar between the PDKO and control mice (Figure 1C–E). Interestingly, PDKO animals meal size was significantly lower during dark phase (-28%; $P<0.001$) due to a slower eating rate (-40%; $P<0.001$) and a longer satiety ratio (+31%; $P<0.001$) (Figure 1F–H).

In order to explain that the weight of the PDKO and control animals were similar despite the differences in food intake, we analyzed the metabolism and behavior of PDKO mice at age 12-16 weeks in an open-flow indirect calorimeter (Oxylet System, Panlab). Indirect calorimetry revealed that PDKO mice had decreased metabolic rate which was reflected by reduction of light and dark phases VO_2 consumption (-8% and -12%, respectively; $P<0.05$) and dark phase VCO_2 production (-17%; $P<0.05$) (Figure 2A-B). These changes were reflected in the energy expenditure which was lower in PDKO mice compared to control animals during the day and night period (-17% and -20%, respectively; $P<0.05$) (Figure 2C).

This lower energy expenditure, was mainly due to a lower use of lipids, as highlighted by the calculated amount of lipid oxidized which was decreased in PDKO mice compared to

6

control animals (Figure 2E). The amount of glucose oxidized was similar in PDKO and control groups (Figure 2F). The decrease in metabolic rate and energy expenditure could not be attributed to alteration in locomotor activity that was similar in both groups (Figure 2D).

The basal metabolic rate (BMR) is the most important part of energy expenditure and then can be involved in the lower energy expenditure observed in PDKO mice compared to control animals. By means of methods described by Meyer et al., we evaluated the BMR in PDKO and control mice. The BMR of PDKO mice was lower than the BMR of control animals (24.51 ± 3.72 and 32.47 ± 3.71 mL O_2/hour for PDKO and control mice, respectively).

Leptin signaling in the arcuate neurons of the PDKO mice

The differences of feeding behavior and energy expenditure in PDKO mice could be explained by a defect in leptin signaling in POMC neurons. To evaluate whether leptin signaling in hypothalamic POMC neurons was modified in mutant mice, we analyzed STAT3 phosphorylation in PDKO and control littermates mice. Leptin was injected i.p. at doses of 5 mg/kg in food-deprived mice, and 30 min later, STAT3 phosphorylation was evaluated by immunofluorescence microscopy. As indicated by the representative photomicrographs shown in Figure 3A and quantification in Figure 3B, the number of pSTAT3-positive neurons is higher in the ARC of PDKO than in the control animals (1293 ± 14 and 1010 ± 59, respectively; $P<0.01$). Very few cells were detected in saline-treated PDKO and control animals (8 ± 1 and 9 ± 2, respectively). Double immunostaining for pSTAT3 and GFP showed that in PDKO mice, pSTAT3 was found in POMC neurons and that $54.3 \pm 1.8\%$ of POMC neurons were positive for pSTAT3 (Figure 3C). Less POMC neurons expressed pSTAT3 after leptin treatment in control animals ($29.7 \pm 1.8\%$) (Figure 3C).

In addition, plasma leptin levels were similar in PDKO and control mice (2.17 ± 0.13 µg/ml and 2.44 ± 0.6 µg/ml, respectively).

The brow adipose tissue (BAT) activity in PDKO mice

In order to investigate whether the increase of leptin sensitivity in POMC neurons enhanced the BAT activity, we assessed the expression of genes involved thermogenesis and fatty acid oxidation. The levels of uncoupling protein 1 (*Ucp1*) and deiodinase 2 (*Dio2*), markers of thermogenic activity, were over-expressed in 16-week-old PDKO mice compared to control animals (+173%, +44%, respectively; *P*<0.05) (Figure 4). In addition, the expression of genes promoting fatty acid oxidation, such as the peroxisome proliferator-activated receptor α (*Pparα*), the PPARγ coactivator 1 family (*Pgc1α* and *β*), the carnitine palmitoyl-transferase I β (*Cpt1β*), the medium- and long-chain acyl-CoA dehydrogenases (*Mcad* and *Lcad*) was evaluated in the BAT of PDKO and control mice. We observed an up-regulation of *Pparα*, *Pgc1α*, and *Mcad* mRNAs in PDKO mice compared to control animals (+180, *P*<0.01, +84%; and +49%; *P*<0.05, respectively) (Figure 4).

The development of the hypothalamus in the control and PDKO mice

The total absence of *Dicer* in POMC-positive neurons led to hyperphagia [27] or a decrease of energy expenditure without an increase of food intake [28]. These defects were associated with the loss of POMC neurons of the arcuate nucleus [27,28]. To directly test the integrity of the POMC neurons in PDKO mice model, the Z/EG conditional reporter alleles[33] were used for the detection of Cre mediated recombination by the induction of eGFP expression. The quantitative analysis revealed that the number of POMC neurons are similar in the arcuate nucleus of PDKO mice compared to control littermates at 16 weeks (222.5±4.5 and 232.5±1.5, respectively) (Figure 5A-C). These results showed that the absence of one allele of *Dicer* gene does not alter POMC neurons survival. Hypothalamic *Pomc* mRNA contents did not differ between mutants and controls animals (Figure 5D). We also observed that the expression of *Lepr*, *Npy*, *Agrp*, *Cart* and *Mc4-r* in the hypothalamus was also unchanged in PDKO and control littermates (Figure 5D). Importantly, we observed an increase of POMC/β-

endorphin protein levels in the hypothalamus of PDKO mice compared to control animals

(+96%; *P*<0.05) (Figure 5E).

Discussion

It has been established that components of the miRNA biogenesis machinery have been associated with energy homeostasis. For instance, transcriptomic analysis of the anorexia mouse model *anx/anx* revealed a tissue specific dysregulation of genes targeted by miRNAs [33]. Particularly, in the hypothalamus, an up-regulation of miRNA-induced silencing complex genes (*Ago2, Pabpc1, Fmr1, Dgcr8*, and *Ddx6*) has been observed. The potential role of miRNAs in the central control of energy homeostasis has been evaluated using conditional Dicer knock-out mice. For instance, the neuron-specific deletion of *Dicer* induced severe and highly reproducible obesity [25]. In the hypothalamus, adult deletion of *Dicer* in the ARC caused hyperphagia and obesity [26]. Interestingly, the deletion of *Dicer* in POMC-expressing cells led to obesity associated with a postnatal ablation of POMC neurons [27,28]. In these models, the absence of *Dicer* in POMC-positive neurons led to hyperphagia [27] or a decrease of energy expenditure without an increase of food intake [28]. In contrast with these results, we observed that mice with the inactivation of one allele of *Dicer* exhibited a normal body weight but a decrease of food intake. Interestingly, indirect calorimetry revealed that PDKO mice had decreased energy expenditure by reduction of VO_2 consumption and CO_2 production which could explain that PDKO mice have normal weight while eating less. In our model, these metabolic defects were not associated with impairment in the number of POMC neurons in ARC of the hypothalamus or a modification in the expression of the melanocortin pathway genes as well as a modification of the physical activity. We observed that the body weight of the control and PDKO animals are similar despite the differences in food intake. As indicated above, this phenotype depends on a decrease in energy expenditure. This difference cannot be explained by the thermogenesis or the fatty acid oxydation in BAT. However, the total energy expenditure includes physical activity (20-40%), thermogenesis (5-10%) and BMR (60-70%) [34,35]. Then the main component of energy expenditure is BMR that is lower in PDKO mice than control animals. Further investigations are required to identify the determinants of this

difference in BMR values between PDKO and control mice. Interestingly, melanocortin system and leptin are ainvolved in the control of cardiovascular system that is one component of BMR.[36]

There is now clear evidence that α-melanocyte-stimulating hormone (α-MSH), one of the major neuropeptides produced by POMC neurons of the ARC, exerts a potent anorexigenic activity [6]. Central administration of α-MSH reduces food intake and body weight through activation of the hypothalamic melanocortin MC3 and MC4 receptor subtypes [9,10,37–39]. In absence of one allele of *Dicer* in POMC cells, we observed a decrease in daily food intake. However, this disturbance in feeding behavior is not associated with an increase in the expression of POMC in the ARC. However, using an antibody against POMC/β-endorphin, we observed an increase in the expression of β-endorphin, one of the major POMC-derived neuropeptides, in the hypothalamus of PDKO mice compared to control animals. In accordance with this result, it has been established that leptin modulates the expression of the enzymes involved in the POMC processing [40]. This observation could indicate that an increase of the biosynthesis or the release of α-MSH can decrease the food intake in PDKO mice compared to control animals. We also can not exclude an increase of POMC stability in PDKO mice. In the present study, we observed that food intake was reduced in PDKO mice model due to decreases in nocturnal meal size and eating rate. Regulation of meal size involves satiation signals originating from the digestive tract and integration of adiposity signals, such as leptin which modulates the effect of satiation signals [41,42]. Following these observations, we propose that this abnormal feeding behavior is secondary to a leptin signaling enhancement in the hypothalamus. In accordance with this hypothesis, we observed an increase of leptin sensitivity in the hypothalamic POMC neurons of PDKO mice which could explain the decrease of food intake in this model. To confirm this hypothesis, we also measured the activity of BAT in PDKO and control mice. In fact, the involvement of the hypothalamic melanocortin system in the regulation of thermogenesis has been shown in

several studies in which chronic central administration of MC4-R agonist or antagonist affected oxygen consumption [43–45]. In addition, neurons of the ARC are in polysynaptic contact with BAT, which is involved in heat production [46,47]. More precisely, POMC-induced stimulation of BAT thermogenesis occurs following downstream melanocortin activation of sympathetic projections via MC4-R-expressing neurons located in the paraventricular nucleus of the hypothalamus and hindbrain [47–49]. In addtion, it has been clearly established that leptin increase thermogenesis and body temperature through activation of the POMC neurons and then the sympathetic nerves that control BAT activity [1,47,49]. In PDKO mice, we observed the induction of the expression of genes controlling fatty acid oxidation (*Pparα, Pgc1α* and *Mcad*) as well as thermogenesis (*Dio2* and *Ucp1*). Together, these data suggested that the miRNAs in POMC neurons are involved in a global fatty acid oxidative program and thermogenesis dependent of leptin. In accordance with this hypothesis, a recent study showed that the *ob/ob* mice have decreased thermogenic markers (β3-adrenergic receptor, PGC1α and UCP1) associated with reduced gene expression related to fatty acid synthesis, mobilization, and oxidation [50].

Altogether, these results indicate that Dicer and Dicer-derived miRNAs are essential for the integrity of leptin signaling in the hypothalamus. In the same line of this conclusion, Crépin et al. indicated that *Irs-2* and *Lepr* are direct targets of miR-200a. The central inhibition of miR-200a ameliorated the metabolic alterations of *ob/ob* mice and normalized the expression of *Irs-2* and *Lepr* [29]. In the same way, Vinnikov et al. found that intracerebroventricular injection of miR-103 mimic attenuated the obesogenic phenotype of mice lacking *Dicer* in forebrain neurons [26]. This effect was mediated by the ability of miR-103 to modulate hypothalamic PI3K-Akt-mTOR activity involved in the insulin and leptin signaling pathways. Recently, numerous studies identified several miRNAs expressed in the hypothalamic neuronal subpopulations involved in the regulation of energy homeostasis. Herzer et al. identified miR-7a as a hypothalamic-enriched miRNA with a high expression in

Neuropeptide Y/Agouti-related peptide neurons which exert an orexigenic effect [51]. In our group, we demonstrated that miR-383, miR-384-3p and miR-488 targeting POMC 3'UTR are expressed in POMC neurons of ARC [30]. Interestingly, it has been shown that Dicer expression in the hypothalamus can be modulated by nutrient and genetic obesity. Particularly, it has been established that Dicer is up-regultaed by fasting [27]. In contrast, there is a decrease of Dicer expression in *ob/ob* and diet-induced obesity models [27]. These results suggested a potential physiological role for Dicer and miRNA biogenesis in the regulation of energy homeostasis. Interestingly, two extreme conditions of nutritional stress, *i.e.* caloric restriction and high fat diet-induced obesity, modified the hypothalamic pattern of expression of a set of miRNAs including let7a, miR-9, miR-30e, miR-132, miR-145, miR-200a and miR-218 [52]. Collectively, these different studies point to the importance of Dicer and Dicer-derived miRNAs as regulators and sensors of central energy homeostasis.

In summary, we observed that the absence of one allele of *Dicer* in POMC neurons leads to defect in feeding behavior in large part through enhanced leptin sensitivity by hypothalamic neurons. The current results show that Dicer and Dicer-derived miRNAs may be involved in the modulation of this complex biological process. In future studies, using an inducible CRISPR/Cas9 system to invalidate DICER or specific miRNAs in POMC neurons of adult brain will allow a better understanding of the role of hypothalamic miRNAs in the control of food intake behaviour.

Material and methods

Animals

To obtain PDKO mice (*Dicer$^{loxP/+}$; PomcCre*), we crossed mice transgenic for *Cre* driven by the *Pomc* promoter with mice carrying the *floxPed-Dicer* allele (*Dicer$^{loxP/loxP}$*) (provided by Pr B Thorens and Pr D Gatfield, University of Lausanne, Switzerland, Pr CJ Tabin, Harvard Medical School, USA and Pr JK Elmquist, University of Texas, USA). For visualising POMC cells, PDKO mice were crossed with the conditional Z/EG reporter transgenic mice (provided by Dr P Durbec, Aix-Marseille Université, France) [53]. *Cre* transgene was detected using the forward primer 5'- CGTACTGACGGTGGGAGAAT -3' and the reverse primer 5'- CCCGGCAAAACAGGTAGTTA -3'. For *Dicer* allele, we used the forward primer 5'- AATATTAATCCTGACAGTGAC -3' and the reverse primer 5'- AAACATGACTCTTCAACTCAAA -3', with the following PCR conditions: 5 min at 95°C, 36 cycles at 95°C for 30 seconds, 62°C for *Cre* or 57°C for *Dicer* for 30 seconds and 72°C for 40 seconds, followed by a final step at 72°C for 7 min. The amplicon size was 166 pb for *Cre*. The amplicon for *Dicer$^{+/+}$* was 351 pb and for *Dicer$^{loxP/loxP}$* 420 pb. For the eGFP we used the same PCR conditions of tau-topaz GFP.

All animals were individually housed in a pathogen-free facility at controlled temperature on a 12/12 hours light/dark cycle (lights from 0700 h to 1900 h) with standard pellet diet (AO4) and water available *ad libitum*. All experiments were conducted in conformity with the rules set by the EC Council Directive (2010/63/UE) and the French 'Direction Départementale de la Protection des Populations des Bouches-du-Rhône' (Licence no. 13.435 and no. 13.430). Protocols used are in agreement with the rules set by the Comité d'Ethique de Marseille, our local Committee for Animal Care and Research. Every precaution was taken to minimise animal stress and the number of animals used.

Physiological studies

The body weights of PDKO and control male mice were measured weekly. PDKO mice and control littermates were used for simultaneous assessments daily changes in food intake and whole-body metabolic profile in an open-flow indirect calorimeter (Oxylet System, Bioseb, France) as described previously [54,55]. Data were collected for two days to confirm acclimation to the calorimetry chambers (stable body weight and food intake), and data from the third day were analyzed. Rates of oxygen consumption (VO_2, ml/min/kg$^{0.75}$) and carbon dioxide production (VCO_2, ml/min/kg$^{0.75}$) were measured for each chamber every 36 min throughout the studies. Energy expenditure (in kcal/day/kg$^{0.75}$ = $1.44 \times VO_2 \times [3.815 + 1.232 \times (VCO_2/VO_2)]$), glucose oxidation (in g/min/kg$^{0.75}$ = $[(4.545 \times VCO_2) - (3.205 \times VO_2)]/1000$), and lipid oxidation (in g/min/kg$^{0.75}$ = $[1.672 \times (VO_2 - VCO_2)]/1000$) were calculated. Total activity was evaluated by summing spontaneous activity, measured in indirect calorimetric cages (Oxylet System, Bioseb, France) and was normalized to the control value. The BMR was evaluated by method described previously by the group of M. Tschöp [34]. For the meal pattern analysis, only meals strictly superior to 0.02 g and composed of one or several bouts separated by less than 5 min were considered in the meal pattern analysis.

Leptin (5 mg/kg, Preprotech) was injected in 24 h food-deprived mice. ELISA kit was used to determine plasma leptin (Alpco, Salem, NH).

Immunohistochemistry

Detection of GFP in PDKO; Z/EG mice was performed on serial hypothalamic 20 μm sections cut from -1.34 mm to -2.70 mm relative to bregma. Animals were perfused intracardially with heparin 10% in phosphate buffer saline (0.1% PBS, 0.1 M, pH 7.4) followed by 4% PFA in PBS maintained at 4°C under ketamine/xylazine anesthesia (100 and 15 mg/kg, respectively). The brains were removed and postfixed for 2 hours in 4% PFA, cryoprotected for 48 hours in 30% sucrose in PBS at 4°C and frozen in O.C.T. (Tissue-Tek, Sakura Finetek, USA). Subsequently the brains were sliced at 20 μm thickness using a

cryostat (Leica CM3050) and transferred serially on gelatin-coated SuperFrost slides (Fisher).

Slides were stored at -20°C until immunohistochemestry. Slices were dried at 37°C and

rehydrated with PBS 3 times 10 min then they were incubated during 1hour in the blocking

solution with 5% horse serum, 0.05% triton X-100 in PBS. After three washes, sections were

incubated over night at 4°C with a polyclonal rabbit primary antibody raised against GFP

(1:10 000, Dr T. Doan, Laboratoire de Chimie Bactérienne-CNRS, Marseille, France).

Sections were washed in PBS 3 times for 10 min and incubated for 1.5 hours with an Alexa

488 fluor-conjugated goat anti-rabbit (1:500, Ref: A11008, Life Technologies).

Detection of pSTAT3 was performed on serial hypothalamic 20-μm sections cut from

−1.34 mm to −2.70 mm relative to the bregma. After rinsing in 0.02 M KPBS, the sections

were pretreated for 20 min with 0.02 M KPBS (pH 7.4) containing 0.3% NaOH and 0.3%

H_2O_2, then with glycine buffer (0.3% glycine in 0.02 M KPBS) for 10 min. After rinsing, the

sections were treated with 0.03% SDS in 0.02 M KPBS, then preincubated for 30 min at room

temperature with 0.02 M KPBS (pH 7.4) containing 1% BSA, 0.4% Triton X-100, and 4%

NGS. Sections were incubated for 48 h at 4°C with a rabbit polyclonal antibody to pSTAT

(1:500; Ref: 9145, Cell Signaling, Beverly, MA). After washing, the sections were then

incubated for 90 min with goat anti-rabbit immunoglobulin-Alexa 594 conjugate (1:500; Ref:

A11012, Life Technologies).

In all conditions, sections were finally coverslipped with mounting medium for

fluorescence microscope preparation. Sections were observed using a Zeiss LSM 700

confocal microscope associated to ZEN 2012 software or a DXM 1200 Camera (Nikon)

coupled to ACT-1 software. For quantitative analysis, cells were counted manually using the

Image J analysis system (National Institutes of Health). For the quantification of pSTAT3-

immunopositive cells and eGFP-positive neurons in PDKO; Z/EG and control mice, the

average number of cells counted in 8 identical sections (from −1.34 mm to −2.70 mm relative

to the bregma) for the hypothalamus in each mouse (n=4) was used for statistical

comparisons. For sections stained for both eGFP and pSTAT3, double-labeled cells were counted by eye, by two different investigators blinded to the treatments. Double-labeled cells were examined at multiple focal levels and at multiple magnifications to ensure that single cells were indeed immunoreactive for both eGFP and pSTAT3.

Quantitative RT-PCR (qRT-PCR) analysis

Mice were killed by decapitation and the hypothalami were collected and frozen in liquid nitrogen and stored at -80°C until RNA extraction. Total RNA was extracted with TRI Reagent (Sigma-Aldrich) as described previously [56]. For RNA quantification, cDNA was synthetized by 2 μg total RNA with M-MLV Reverse Transcriptase (Promega Corporation). For real-time PCR, we used LightCycler 480 (Roche). Primer sequences used to detect the mRNA levels are listed in Table 1. PCR was initiated by one cycle of 95ºC for 10 min, followed by 40 cycles of 10 seconds at 95ºC, 30 seconds at 60ºC, and 2 seconds at 72ºC, followed by a holding at 40°C.

Western Blotting

The hypothalami were collected from PDKO and control animals. Tissue lysates were prepared by mashing in cold lysis buffer (50 mM Tris pH 7.9, 150 mM NaCl, 5 mM EDTA, 25 mM NaF, 1% Igepal, 0.5% Na deoxycholate, 0.1% SDS, 1 mM DTT, 2mM Na_3VO_4, 6.4 mg/ml PNPP, Protease Inhibitor Cocktail (Sigma-Aldrich)). A sample of lysate (40 μg) was boiled in 30 μl of Laemmli 2x Concentrate Sample Buffer (Sigma-Aldrich) for 5 min and then cooled in ice. 40 μg of total protein were separated by 15% SDS-polyacrylamide gel electrophoresis and transferred to polyvinylidene fluoride membranes (450 mA, 105 min). Membranes were blocked with 10% fat-free milk in Tris-buffered saline containing 0.1% Tween 20 (TBST) buffer (50 mM Tris-HCl, pH 7.5, 138 mM NaCl, and 0.1% Tween 20) and were subsequently incubated with the following primary goat anti-POMC/endorphin antibody

(1:1000, Ref: ab32893, Abcam) or mouse anti-β-actin (1:4000, Ref: G8795, Sigma) and this

antibody was incubated at 4 °C overnight. Then, the membranes were washed with TBST and

incubated for 2 hours with horseradish peroxidase-conjugated secondary antibody (1:10000,

Jackson Immunoresearch). Band were developped on membrane using the 1-Step Ultra TMB-

Blotting Solution (Thermo Scientific).

Statistical analysis

All data are expressed as mean ± SEM. Statistical analysis was performed by using GraphPad

6.0 software, with repeated measures ANOVA followed by Bonferroni's multiple

comparisons for body weight and cumulative food intake. All other parameters were analyzed

using unpaired 2-tailed Mann-Whitney test. $P < 0.05$ was considered significant.

Acknowledgments

Funding

References

1.   Derghal A, Djelloul M, Trouslard J, Mounien L. The Role of MicroRNA in the Modulation of the Melanocortinergic System. Front Neurosci 2017; 11:181.

2.   Cowley MA, Smart JL, Rubinstein M, Cerdán MG, Diano S, Horvath TL, Cone RD, Low MJ. Leptin activates anorexigenic POMC neurons through a neural network in the arcuate nucleus. Nature 2001; 411:480–4.

3.   Ibrahim N, Bosch MA, Smart JL, Qiu J, Rubinstein M, Rønnekleiv OK, Low MJ, Kelly MJ. Hypothalamic proopiomelanocortin neurons are glucose responsive and express K(ATP) channels. Endocrinology 2003; 144:1331–40.

4.   Plum L, Belgardt BF, Brüning JC. Central insulin action in energy and glucose homeostasis. J Clin Invest 2006; 116:1761–6.

5.   Parton LE, Ye CP, Coppari R, Enriori PJ, Choi B, Zhang C-Y, Xu C, Vianna CR, Balthasar N, Lee CE, et al. Glucose sensing by POMC neurons regulates glucose homeostasis and is impaired in obesity. Nature 2007; 449:228–32.

6.   Mounien L, Do Rego J-C, Bizet P, Boutelet I, Gourcerol G, Fournier A, Brabet P, Costentin J, Vaudry H, Jégou S. Pituitary adenylate cyclase-activating polypeptide inhibits food intake in mice through activation of the hypothalamic melanocortin system. Neuropsychopharmacol Off Publ Am Coll Neuropsychopharmacol 2009; 34:424–35.

7.   Mounien L, Marty N, Tarussio D, Metref S, Genoux D, Preitner F, Foretz M, Thorens B. Glut2-dependent glucose-sensing controls thermoregulation by enhancing the leptin sensitivity of NPY and POMC neurons. FASEB J Off Publ Fed Am Soc Exp Biol 2010; 24:1747–58.

8.   Hill JW, Elias CF, Fukuda M, Williams KW, Berglund ED, Holland WL, Cho Y-R, Chuang J-C, Xu Y, Choi M, et al. Direct insulin and leptin action on pro-opiomelanocortin neurons is required for normal glucose homeostasis and fertility. Cell Metab 2010; 11:286–97.

9.   Huszar D, Lynch CA, Fairchild-Huntress V, Dunmore JH, Fang Q, Berkemeier LR, Gu W, Kesterson RA, Boston BA, Cone RD, et al. Targeted disruption of the melanocortin-4 receptor results in obesity in mice. Cell 1997; 88:131–41.

10.   Yaswen L, Diehl N, Brennan MB, Hochgeschwender U. Obesity in the mouse model of pro-opiomelanocortin deficiency responds to peripheral melanocortin. Nat Med 1999; 5:1066–70.

11.   Lee YS. The role of leptin-melanocortin system and human weight regulation: lessons from experiments of nature. Ann Acad Med Singapore 2009; 38:34–11.

12.   Bouret SG, Draper SJ, Simerly RB. Trophic action of leptin on hypothalamic neurons that regulate feeding. Science 2004; 304:108–10.

13.   Gao Q, Wolfgang MJ, Neschen S, Morino K, Horvath TL, Shulman GI, Fu X-Y. Disruption of neural signal transducer and activator of transcription 3 causes obesity, diabetes, infertility, and thermal dysregulation. Proc Natl Acad Sci U S A 2004; 101:4661–6.

14.   Pinto S, Roseberry AG, Liu H, Diano S, Shanabrough M, Cai X, Friedman JM, Horvath TL. Rapid rewiring of arcuate nucleus feeding circuits by leptin. Science 2004; 304:110–5.

15.   Coupé B, Ishii Y, Dietrich MO, Komatsu M, Horvath TL, Bouret SG. Loss of autophagy in pro-opiomelanocortin neurons perturbs axon growth and causes metabolic dysregulation. Cell Metab 2012; 15:247–55.

16.   Stevens A, Begum G, Cook A, Connor K, Rumball C, Oliver M, Challis J, Bloomfield F, White A. Epigenetic changes in the hypothalamic proopiomelanocortin and glucocorticoid receptor genes in the ovine fetus after periconceptional undernutrition. Endocrinology 2010; 151:3652–64.

17.   Gali Ramamoorthy T, Allen T-J, Davies A, Harno E, Sefton C, Murgatroyd C, White A. Maternal overnutrition programs epigenetic changes in the regulatory regions of hypothalamic Pomc in the offspring of rats. Int J Obes 2005 2018;

18.   Vogt MC, Paeger L, Hess S, Steculorum SM, Awazawa M, Hampel B, Neupert S, Nicholls HT, Mauer J, Hausen AC, et al. Neonatal insulin action impairs hypothalamic neurocircuit formation in response to maternal high-fat feeding. Cell 2014; 156:495–509.

19.   Marco A, Kisliouk T, Tabachnik T, Meiri N, Weller A. Overweight and CpG methylation of the Pomc promoter in offspring of high-fat-diet-fed dams are not "reprogrammed" by regular chow diet in rats. FASEB J Off Publ Fed Am Soc Exp Biol 2014; 28:4148–57.

20.   Bartel DP. MicroRNAs: genomics, biogenesis, mechanism, and function. Cell 2004; 116:281–97.

21.   Derghal A, Djelloul M, Trouslard J, Mounien L. An Emerging Role of micro-RNA in the Effect of the Endocrine Disruptors. Front Neurosci 2016; 10:318.

22.   Esau C, Davis S, Murray SF, Yu XX, Pandey SK, Pear M, Watts L, Booten SL, Graham M, McKay R, et al. miR-122 regulation of lipid metabolism revealed by in vivo antisense targeting. Cell Metab 2006; 3:87–98.

23.   Frost RJA, Olson EN. Control of glucose homeostasis and insulin sensitivity by the Let-7 family of microRNAs. Proc Natl Acad Sci U S A 2011; 108:21075–80.

24.   Grueter CE, van Rooij E, Johnson BA, DeLeon SM, Sutherland LB, Qi X, Gautron L, Elmquist JK, Bassel-Duby R, Olson EN. A cardiac microRNA governs systemic energy homeostasis by regulation of MED13. Cell 2012; 149:671–83.

25.   Mang GM, Pradervand S, Du N-H, Arpat AB, Preitner F, Wigger L, Gatfield D, Franken P. A neuron-specific deletion of the microRNA-processing enzyme DICER induces

severe but transient obesity in mice. PloS One 2015; 10:e0116760.

26.   Vinnikov IA, Hajdukiewicz K, Reymann J, Beneke J, Czajkowski R, Roth LC, Novak M, Roller A, Dörner N, Starkuviene V, et al. Hypothalamic miR-103 protects from hyperphagic obesity in mice. J Neurosci Off J Soc Neurosci 2014; 34:10659–74.

27.   Schneeberger M, Altirriba J, García A, Esteban Y, Castaño C, García-Lavandeira M, Alvarez CV, Gomis R, Claret M. Deletion of miRNA processing enzyme Dicer in POMC-expressing cells leads to pituitary dysfunction, neurodegeneration and development of obesity. Mol Metab 2012; 2:74–85.

28.   Greenman Y, Kuperman Y, Drori Y, Asa SL, Navon I, Forkosh O, Gil S, Stern N, Chen A. Postnatal ablation of POMC neurons induces an obese phenotype characterized by decreased food intake and enhanced anxiety-like behavior. Mol Endocrinol Baltim Md 2013; 27:1091–102.

29.   Crépin D, Benomar Y, Riffault L, Amine H, Gertler A, Taouis M. The over-expression of miR-200a in the hypothalamus of ob/ob mice is linked to leptin and insulin signaling impairment. Mol Cell Endocrinol 2014; 384:1–11.

30.   Derghal A, Djelloul M, Airault C, Pierre C, Dallaporta M, Troadec J-D, Tillement V, Tardivel C, Bariohay B, Trouslard J, et al. Leptin is required for hypothalamic regulation of miRNAs targeting POMC 3'UTR. Front Cell Neurosci 2015; 9:172.

31.   Harfe BD, McManus MT, Mansfield JH, Hornstein E, Tabin CJ. The RNaseIII enzyme Dicer is required for morphogenesis but not patterning of the vertebrate limb. Proc Natl Acad Sci U S A 2005; 102:10898–903.

32.   Balthasar N, Coppari R, McMinn J, Liu SM, Lee CE, Tang V, Kenny CD, McGovern RA, Chua SCJ, Elmquist JK, et al. Leptin receptor signaling in POMC neurons is required for normal body weight homeostasis. Neuron 2004; 42:983–91.

33.   Mercader JM, González JR, Lozano JJ, Bak M, Kauppinen S, Sumoy L, Dierssen M, Fernández-Aranda F, Visa J, Gratacòs M, et al. Aberrant brain microRNA target and miRISC gene expression in the anx/anx anorexia mouse model. Gene 2012; 497:181–90.

34.   Meyer CW, Reitmeir P, Tschöp MH. Exploration of Energy Metabolism in the Mouse Using Indirect Calorimetry: Measurement of Daily Energy Expenditure (DEE) and Basal Metabolic Rate (BMR). Curr Protoc Mouse Biol 2015; 5:205–22.

35.   Tschöp MH, Speakman JR, Arch JRS, Auwerx J, Brüning JC, Chan L, Eckel RH, Farese RV, Galgani JE, Hambly C, et al. A guide to analysis of mouse energy metabolism. Nat Methods 2011; 9:57–63.

36.   do Carmo JM, da Silva AA, Dubinion J, Sessums PO, Ebaady SH, Wang Z, Hall JE. Control of metabolic and cardiovascular function by the leptin-brain melanocortin pathway. IUBMB Life 2013; 65:692–8.

37.   Fan W, Boston BA, Kesterson RA, Hruby VJ, Cone RD. Role of melanocortinergic

neurons in feeding and the agouti obesity syndrome. Nature 1997; 385:165–8.

38.   Butler AA, Kesterson RA, Khong K, Cullen MJ, Pelleymounter MA, Dekoning J, Baetscher M, Cone RD. A unique metabolic syndrome causes obesity in the melanocortin-3 receptor-deficient mouse. Endocrinology 2000; 141:3518–21.

39.   Chen AS, Marsh DJ, Trumbauer ME, Frazier EG, Guan XM, Yu H, Rosenblum CI, Vongs A, Feng Y, Cao L, et al. Inactivation of the mouse melanocortin-3 receptor results in increased fat mass and reduced lean body mass. Nat Genet 2000; 26:97–102.

40.   Pritchard LE, Turnbull AV, White A. Pro-opiomelanocortin processing in the hypothalamus: impact on melanocortin signalling and obesity. J Endocrinol 2002; 172:411–21.

41.   Flynn MC, Scott TR, Pritchard TC, Plata-Salamán CR. Mode of action of OB protein (leptin) on feeding. Am J Physiol 1998; 275:R174-179.

42.   Smith GP. The controls of eating: a shift from nutritional homeostasis to behavioral neuroscience. Nutr Burbank Los Angel Cty Calif 2000; 16:814–20.

43.   Baran K, Preston E, Wilks D, Cooney GJ, Kraegen EW, Sainsbury A. Chronic central melanocortin-4 receptor antagonism and central neuropeptide-Y infusion in rats produce increased adiposity by divergent pathways. Diabetes 2002; 51:152–8.

44.   Small CJ, Liu YL, Stanley SA, Connoley IP, Kennedy A, Stock MJ, Bloom SR. Chronic CNS administration of Agouti-related protein (Agrp) reduces energy expenditure. Int J Obes Relat Metab Disord J Int Assoc Study Obes 2003; 27:530–3.

45.   Yasuda T, Masaki T, Kakuma T, Yoshimatsu H. Hypothalamic melanocortin system regulates sympathetic nerve activity in brown adipose tissue. Exp Biol Med Maywood NJ 2004; 229:235–9.

46.   Cano G, Passerin AM, Schiltz JC, Card JP, Morrison SF, Sved AF. Anatomical substrates for the central control of sympathetic outflow to interscapular adipose tissue during cold exposure. J Comp Neurol 2003; 460:303–26.

47.   Voss-Andreae A, Murphy JG, Ellacott KLJ, Stuart RC, Nillni EA, Cone RD, Fan W. Role of the central melanocortin circuitry in adaptive thermogenesis of brown adipose tissue. Endocrinology 2007; 148:1550–60.

48.   Williams DL, Bowers RR, Bartness TJ, Kaplan JM, Grill HJ. Brainstem melanocortin 3/4 receptor stimulation increases uncoupling protein gene expression in brown fat. Endocrinology 2003; 144:4692–7.

49.   Song CK, Vaughan CH, Keen-Rinehart E, Harris RBS, Richard D, Bartness TJ. Melanocortin-4 receptor mRNA expressed in sympathetic outflow neurons to brown adipose tissue: neuroanatomical and functional evidence. Am J Physiol Regul Integr Comp Physiol 2008; 295:R417-428.

50.   Martins FF, Bargut TCL, Aguila MB, Mandarim-de-Lacerda CA. Thermogenesis, fatty acid synthesis with oxidation, and inflammation in the brown adipose tissue of ob/ob (-/-) mice. Ann Anat Anat Anz Off Organ Anat Ges 2017; 210:44–51.

51.   Herzer S, Silahtaroglu A, Meister B. Locked nucleic acid-based in situ hybridisation reveals miR-7a as a hypothalamus-enriched microRNA with a distinct expression pattern. J Neuroendocrinol 2012; 24:1492–504.

52.   Sangiao-Alvarellos S, Pena-Bello L, Manfredi-Lozano M, Tena-Sempere M, Cordido F. Perturbation of hypothalamic microRNA expression patterns in male rats after metabolic distress: impact of obesity and conditions of negative energy balance. Endocrinology 2014; 155:1838–50.

53.   Novak A, Guo C, Yang W, Nagy A, Lobe CG. Z/EG, a double reporter mouse line that expresses enhanced green fluorescent protein upon Cre-mediated excision. Genes N Y N 2000 2000; 28:147–55.

54.   Dominguez JF, Guo L, Carrasco Molnar MA, Ballester Escobedo A, Dunphy T, Lund TD, Turman JEJ. Novel indirect calorimetry technology to analyze metabolism in individual neonatal rodent pups. PloS One 2009; 4:e6790.

55.   Marcotorchino J, Tourniaire F, Astier J, Karkeni E, Canault M, Amiot M-J, Bendahan D, Bernard M, Martin J-C, Giannesini B, et al. Vitamin D protects against diet-induced obesity by enhancing fatty acid oxidation. J Nutr Biochem 2014; 25:1077–83.

56.   Karkeni E, Bonnet L, Astier J, Couturier C, Dalifard J, Tourniaire F, Landrier J-F. All-trans-retinoic acid represses chemokine expression in adipocytes and adipose tissue by inhibiting NF-κB signaling. J Nutr Biochem 2017; 42:101–7.

LEGENDS TO FIGURES

Table 1. Sequence of the oligonucleotides used for quantitative RT-PCR amplification

Figure 1. Body weight and feeding behavior in PDKO and control animals. 12-16-week-old male PDKO and control mice were analyzed in metabolic cages. (A) Mean body weight, (B) Mean cumulative food intake, (C) number of meals, (D) duration of meals, (E) intermeal, (F) meal size, (G) eating rate, (H) satiety are given for the dark phase and light phase in male PDKO and control mice. Values represent the mean ± SEM (n=6). *, $P<0.05$; ***, $P<0.001$ *vs* control.

Figure. 2. Impaired energy expenditure in PDKO mice. 12-16-week-old male PDKO and control mice were analyzed in metabolic cages. (A) Area under curve (AUC) average oxygen consumption per 30 min during light/dark cycle, (B) AUC average carbon dioxide production per 36 min during light/dark cycle, (C) AUC average energy expenditure per 36 min during light/dark cycle, (D) Mean physical activity during light/dark cycle, (E) Lipid oxidation, (F) Carbohydrate oxidation. Values represent the mean ± SEM (n=6). *, $P<0.05$; **$P<0.01$ *vs* control.

Figure 3. **Leptin sensitivity is enhanced in PDKO mice**. (A) Typical pictures illustrating double immunohistochemical detection of eGFP (green) and pSTA3 (red) in the arcuate nucleus from leptin-treated control and PDKO animals. White arrowheads point to neurons expressing eGFP but not pSTAT3 protein. White arrows point to neurons expressing eGFP and pSTAT3 protein. (B) Quantitative analysis of pSTAT3 positive neurons in control and PDKO mice after leptin treatment in the arcuate nucleus. (C) Quantitative analysis of the

percentage of eGFP-positive neurons expressing pSTAT3 protein in the arcuate nucleus from leptin-injected control and PDKO mice. Scale bar = 100 μm. Values represent the mean ± SEM (n=4). *, $P<0.05$, **, $P<0.01$ *vs* control. 3V: third ventricle.

Figure 4. Expression of genes involved thermogenesis and fatty acid oxidation are altered in the BAT of PDKO mice. Gene expression in BAT of PDKO and control mice at 12-16 weeks of age. *Cpt1β*: carnitine palmitoyl-transferase I β; *Dio2*: deiodinase 2; *Mcad* and *Lcad:* medium- and long-chain acyl-CoA dehydrogenases, *Pparα*: peroxisome proliferator-activated receptor α, PPARγ coactivator 1 family (*Pgc1α* and *β*), *Ucp1*: uncoupling protein 1. Values represent mean ± S.E.M (n=7). *, $P<0.05$, **, $P<0.01$ *vs* control.

Figure 5. Melanocortin pathway is not altered in PDKO mice. (A-B) Representative immunofluorescence of Cre-induced GFP expression in the arcuate nucleus of PDKO and control littermates at 16 weeks of age. (C) Quantitative analysis of POMC-positive neurons the arcuate nucleus of PDKO and control littermates at 16 weeks of age. (D) Quantitative analysis of *Pomc*, *leptin and melanocortin receptor*, *Npy*, *Agrp* and *Cart* mRNA levels in the hypothalamus of PDKO and control littermates at 16 weeks of age. (E) Western blot analysis for β-endorphin/POMC expression in the hypothalamus of PDKO and control mice. Scale bar = 100 μm. *Agrp* : agouti related peptide; Arc: arcuate nucleus; *Cart*: cocaine and amphetamin related transcript; *Lepr*: leptin receptor; *Mc4-r*: melanocortin receptor type 4; *Npy*: neuropeptide Y; *Pomc*: pro-opiomelanocortin; 3V: third ventricle. Values represent the mean ± SEM (n=4-6 for A-D and n=3 for E). *, $P<0.05$.

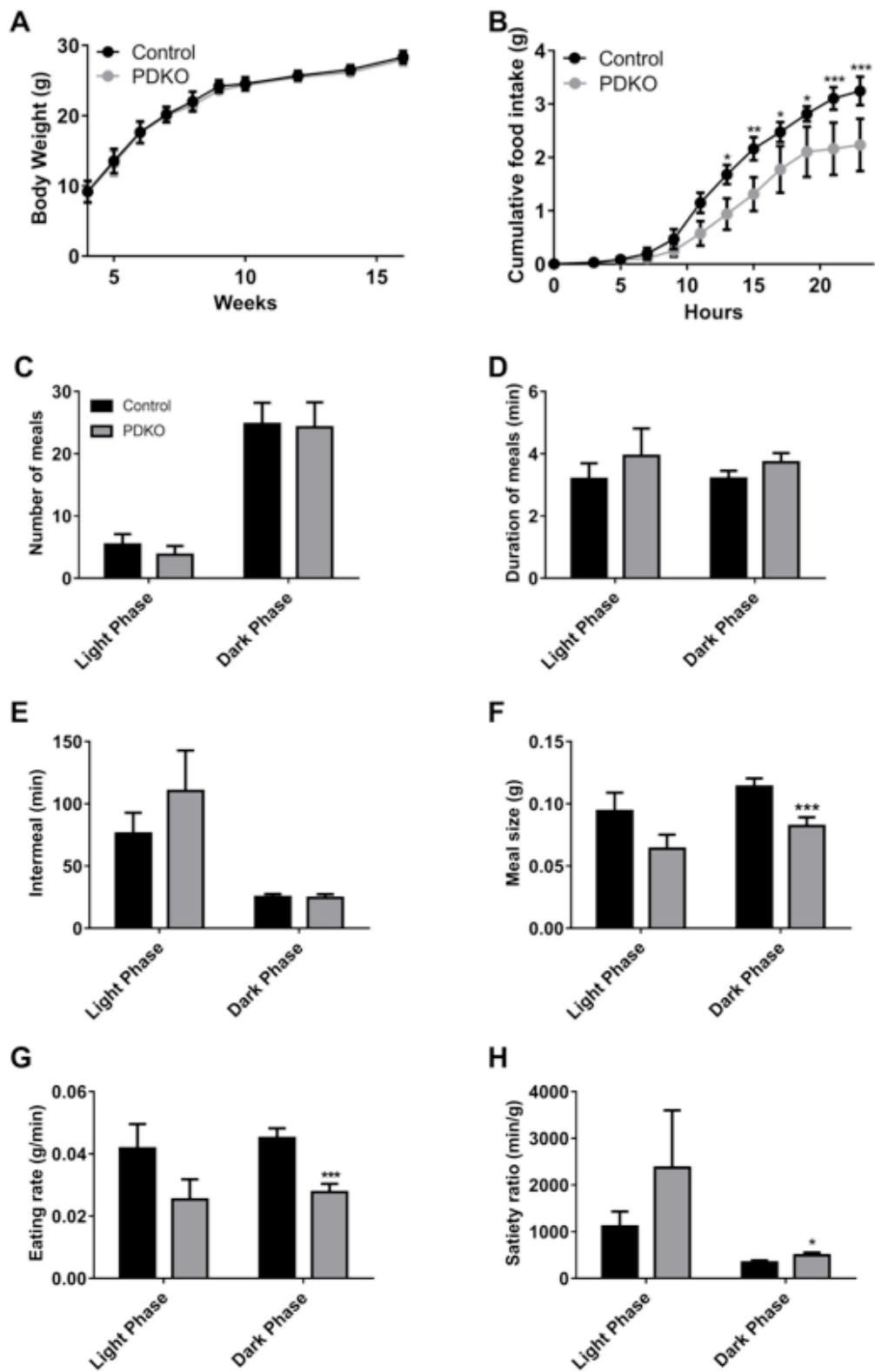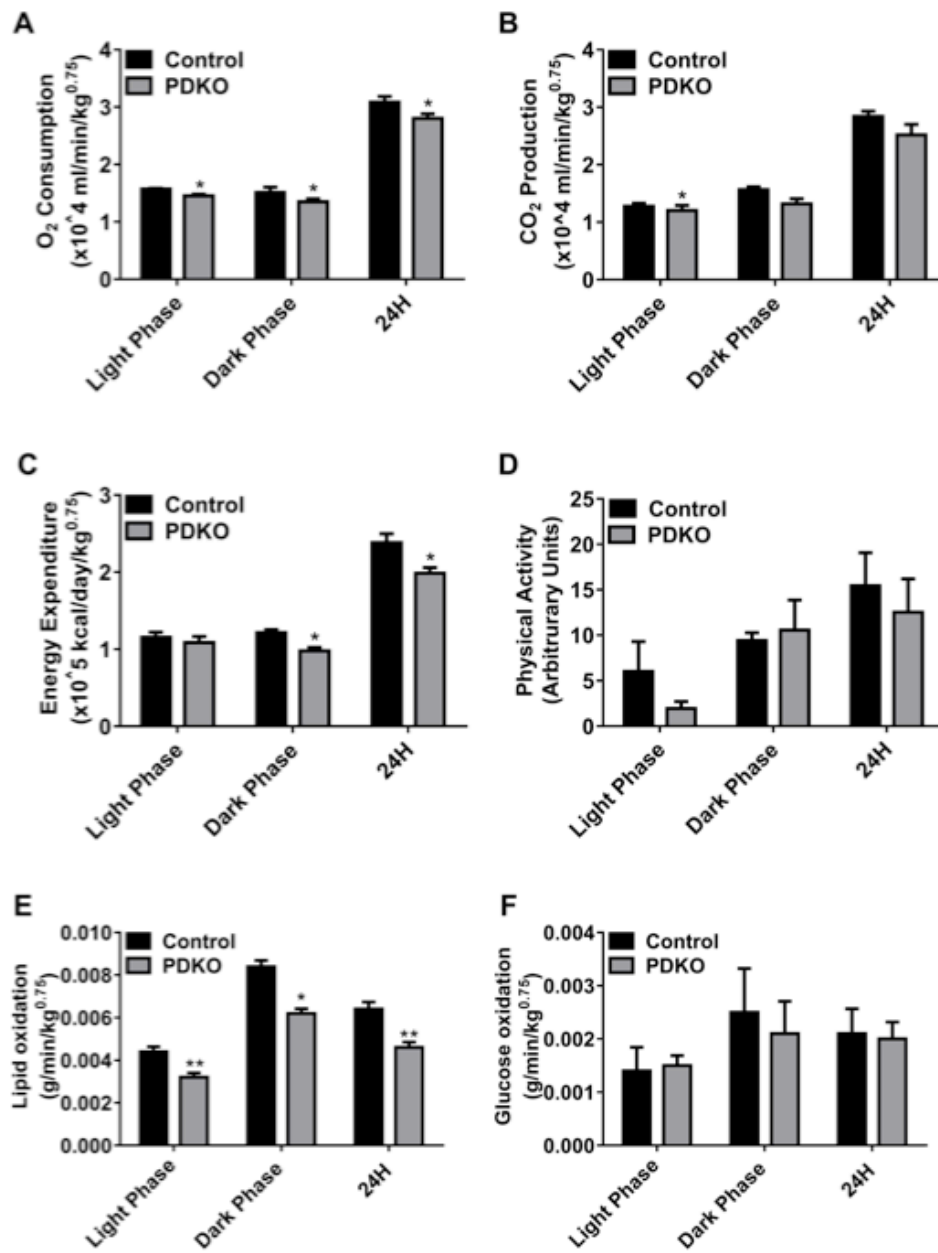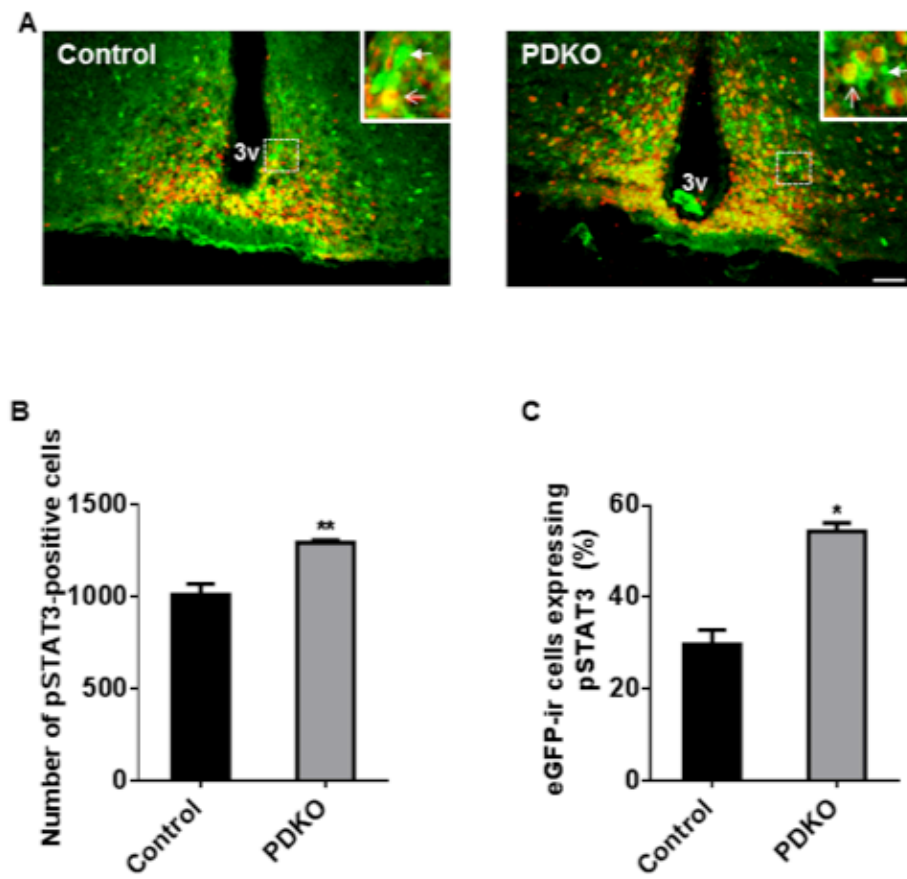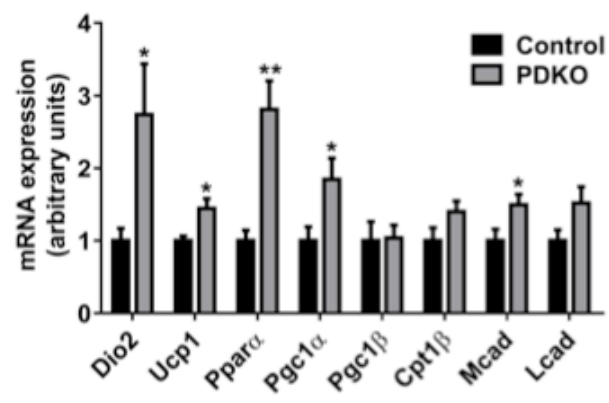**Figure S1. Sex-ratio and percentage of transgenic animals in the progeny of Pomc-Cre+ mated to Dicer^lox/+ mice.**

Figure 1

Figure 2

Figure 3

Figure 4

Figure 5

Figure S1